Rare Metal Materials and Engineering
Volume 52, Issue 4, April 2023
Available online at www.rmme.ac.cn

Science Press

Cite this article as: Wang Pengju, Zhao Shujie, Zhong Ning, et al. Microstructures and Mechanical Properties of AlSn20Cu/Steel Laminated Metal Composites Fabricated by Cold Roll Bonding[J]. Rare Metal Materials and Engineering, 2023, 52(04): 1259-1266.

ARTICLE

Microstructures and Mechanical Properties of AlSn20Cu/Steel Laminated Metal Composites Fabricated by Cold Roll Bonding

Wang Pengju[1,2], Zhao Shujie[2], Zhong Ning[2,3], Yang Qian[2], Wu Bo[2,3], Zhang Peng[2], Du Bing[2], Tang Qian[1]

[1] College of Mechanical and Vehicle Engineering, Chongqing University, Chongqing 400030, China; [2] Chongqing Hongjiang Machinery Co., Ltd, Chongqing 402160, China; [3] Chongqing Yuejin Machinery Co., Ltd, Chongqing 402160, China

Abstract: Laminated metal composites (LMCs) of 1060Al/AlSn20Cu/1060Al/steel were fabricated by cold roll bonding, and the effects of rolling reductions on the microstructure and mechanical properties were characterized. The microstructure was observed by scanning electron microscopy (SEM) and electron backscatter diffraction (EBSD), and the mechanical properties were examined by tensile tests. The initial rolling reduction was 17%, and the minimum stable rolling reduction was 40%. Results show that the increase in rolling reduction causes an elongation of the Sn phases in the AlSn20Cu layer and lengthening of grains in the steel layer along the rolling direction, whereas the 1060Al layers shows equiaxed grains. The tensile strength and interfacial bonding strength of the composite sheets increase while the elongation decreases with increasing rolling reduction. The fracture of the AlSn20Cu layer is related to the Sn phase.

Key words: roll bonding; AlSn20Cu/steel laminated sheet; microstructure; mechanical property

The excellent friction and wear properties of Al-Sn based materials have led to their wide usage in engine sliding wear[1]. The soft Sn phase present in the Al-Sn alloy provides solid lubrication, and also increases other special properties, such as good embedding ability, adaptability and seizure resistance. The most frequently used Al-Sn based sliding wear materials are the high-tin AlSn20Cu alloys[2–3].

The fatigue strength and carrying ability for sliding wear can be improved by bonding the AlSn20Cu alloy with a low-carbon steel. Many methods, including roll bonding, diffusion bonding, explosion welding and friction stir welding, are available for attaining fine interfacial bonding between Al and steel layers. Roll bonding is the commonest, the most convenient and productive method among them[4–6]. Therefore, roll bonding has been a rational choice for the industrial production of Al/steel clad sheets and strips.

Elemental Sn reacts readily with elemental Fe, and this reaction can decrease the Al/steel interfacial bonding strength. A pure Al foil as the barrier is inserted between the AlSn20Cu and steel layers, which separates the rolling process into two parts: the rolling of the pure Al/AlSn20Cu clad sheet, and the rolling of the Al clad sheet to the steel.

The fabrication and properties of Al/steel clad sheets and strips have attracted significant research interest. Manesh et al[7] prepared Al/steel clad sheets using different rolling parameters and found that several processing parameters, including the rolling reduction, rolling speed, internal layer thickness and yield strength, and frictional conditions can greatly impact the interfacial bonding strength. Gao et al[8] fabricated an Al/steel clad sheet by cold roll bonding and explored the influence of surface preparation on the interfacial bonding strength. They found that the bonding strength of the Al/steel clad sheet is higher when the sheet is treated by belt grinding than by wire brushing. Filho et al[9] studied the effect of the interfacial shear mode on the shear strain zone in the Al/steel roll bonding process and concluded that the width of the

Received date: September 12, 2022
Foundation item: National Natural Science Foundation of China (51975073)
Corresponding author: Tang Qian, Ph. D., Professor, College of Mechanical and Vehicle Engineering, Chongqing University, Chongqing 400030, P. R. China, E-mail: tqcqu@cqu.edu.cn

Copyright © 2023, Northwest Institute for Nonferrous Metal Research. Published by Science Press. All rights reserved.

interface shear zone is related to the magnitude of the shear strain and the structural composition of the hybrid material. Kim et al[10] used the finite element method to explore the interfacial bonding strength and shear stress of cold-rolled and annealed Al1050/STS439 clad sheets. Cui et al[11] studied the microstructure and mechanical properties of high-tin aluminium alloy/steel by roll bonding and reported that the bonding strength of Al/steel after annealing at 350 °C for 2 h is 92.4 MPa, which is about 26% higher than that of the rolled state. However, there are few available reports on the effect of rolling reduction on the microstructure and mechanical properties of 1060Al/AlSn20Cu/1060Al/steel laminated metal composites (LMCs).

This study described the fabrication of 1060Al/AlSn20Cu/1060Al/steel LMCs with different rolling reductions through cold roll bonding at room temperature. The evolution of the microstructure of the interfaces and base metals of AlSn20Cu/steel LMCs was investigated, and the effect of rolling reductions on the mechanical properties of laminated composites was explored.

1 Experiment

The raw components of the laminated sheets were 1060Al (1.0 mm in thickness), AlSn20Cu (10.0 mm in thickness) and low-carbon steel (3 mm in thickness); their chemical compositions are given in Table 1 and Table 2. The 1060Al was annealed at 350 °C for 0.5 h and the low-carbon steel was annealed at 600 °C for 2 h. The AlSn20Cu was a cast alloy and used directly without any treatments. The three sheets were cut from their original size to 100 mm×120 mm.

The rolling process was conducted as two separate processes: rolling of the 1060Al/AlSn20Cu clad sheet and rolling of the Al clad sheet/steel. The surfaces of the 1060Al, AlSn20Cu and steel sheets were brushed with a steel brush and then degreased with ethyl alcohol. Sliding between dissimilar metals during the roll bonding process was prevented by riveting the sheets with tacking sequence of 1060Al/AlSn20Cu/1060Al and Al clad sheet/steel. The riveted 1060Al/AlSn20Cu/1060Al sheets were pushed first into the rolling mill and bonded at room temperature. After three rolling treatments, the final thickness of the Al clad sheets was 1.5 mm. The riveted Al/steel sheets were then rolled at room temperature. Single reductions of about 35%, 46% and 57% were achieved at a rolling speed of 0.2 m/s. The fabrication process for the 1060Al/AlSn20Cu/1060Al/steel LMCs is shown in Fig. 1. To explore the deformation zone of the Al/steel clad sheet, a sudden stop was executed during the rolling process with the rolling reduction of 57%.

Table1 Chemical compositions of 1060Al and AlSn20Cu (wt%)

	Al	Mg	Ti	Si	Sn	Fe	Cu	Mn
1060Al	Bal.	0.02	0.03	0.23	-	0.34	0.05	0.03
AlSn20Cu	Bal.	-	0.04	0.06	18.9	0.01	0.98	0.15

Table 2 Chemical composition of low-carbon steel (wt%)

Fe	C	Si	Mn	P	S
Bal.	0.09	0.25	0.30	0.03	0.03

Fig. 2 shows the back scattered electron (BSE) images of the 1060Al/AlSn20Cu clad sheet. No obvious defects or cracks are evident at the 1060Al/AlSn20Cu interface in Fig. 2a, suggesting that the bonding interface is intact. Fig. 2b shows the microstructure of the AlSn20Cu layer. The white phase is Sn and the dark phase is Al. The Sn phase is distributed in a chain shape along the rolling direction.

The LMC samples were cut to a size of 10 mm×8 mm in the transverse direction (TD) plane for the microstructure analysis. The cut samples were then polished mechanically to a mirror-like surface with abrasive paper and diamond polishing paste. The interface and microstructure were characterized by a TSCAN MIRA3 field emission scanning electron microscope (FESEM) equipped with an electron backscatter diffraction (EBSD) detector. The samples for EBSD observation were cut by a wire saw and then ground with abrasive papers, followed by electro-polishing at 20 V for 40 s. The electrolyte was a mixture of perchloric acid and ethyl alcohol (1: 9, v/v). The outermost layer was milled before fabricating the Al-Sn based sliding wear to allow observation of the microstructures of the AlSn20Cu/1060Al/steel part.

The effects of the rolling reductions on the mechanical properties were determined by tensile tests and tensile shear tests performed on a Shimadzu mechanical testing machine at a strain rate of 10^{-3} s^{-1}. Fig. 3 shows the schematic figures for the tensile tests and tensile shear tests of the composite sheets. The h_0 and h_1 represent the thickness of the clad sheet and Al layer in Fig.3b.

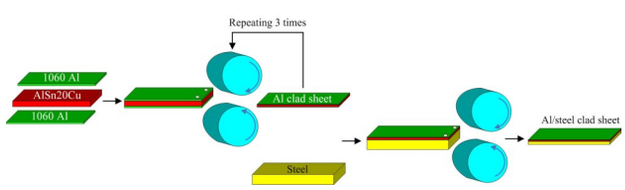

Fig.1 Schematic diagram depicting the cold roll bonding of the 1060Al/AlSn20Cu/1060Al/steel LMCs

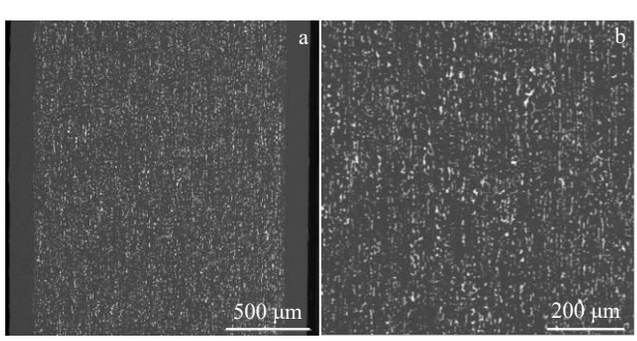

Fig. 2 BSE images of 1060Al/AlSn20Cu clad sheet: (a) 1060Al/AlSn20Cu interface and (b) AlSn20Cu layer

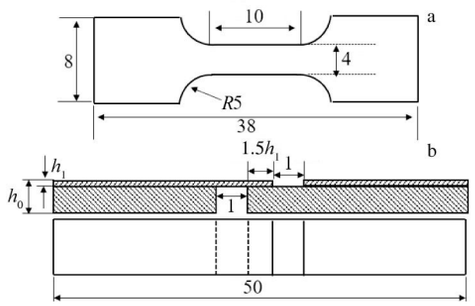

Fig.3 Schematic figures for tensile test (a) and tensile shear test (b) of the LMC

2 Results and Discussion

2.1 Thickness distribution of the Al and steel layers in 1060Al/AlSn20Cu/1060Al/steel LMC

Fig.4 shows the interface morphology and thickness distribution of the deformation zone for the Al/steel LMC. The thickness parameter was measured from the left bonding point to the right exit point of the sample. The results of the thickness distribution and rolling reduction are shown in Fig.4b and 4c. During the rolling process, the thickness of the Al and steel layers decreases. The location of the initial bond reduction is obtained, and the magnified area is marked by the blue arrow in Fig.4a. The initial bonding reduction was 17%, in agreement with previous literature values of 12.5%–25% for the initial bonding reduction[12].

The thickness variations in the Al and steel layers are separated into three main parts: zone between A and B, zone between B and C and zone between C and 0, where point 0 is the rolling exit, point B is the initial bonding reduction and point A is the rolling entrance. In zone between A and B, the thickness change is greater for the Al layer than for the steel layer. In contrast, the reverse occurs in zone between B and C, where a dramatic decrease in the thickness of the steel layer is observed. Zone between C and 0 shows stable changes in the Al and steel layers.

Wang et al[13] used a slice method to explore the interfacial shear stress distribution in the Al/steel deformation zone and found that the thickness distribution of Al and steel layers is mainly related to the rolling pressure and the interfacial shear stress. During the initial rolling stage, the rolling pressure is far greater than the yield strength of the Al layer. The Al layer thus undergoes drastic plastic deformation and the thickness decreases sharply in zone between A and B. Because point B is the site of the initial bonding reduction, zone between B and C is the bonded region.

The interfacial bonding strength increases with increasing rolling reduction[14]. In the initial bonding zone between B and C, the interfacial bonding strength is smaller than the interfacial shear stress. The Al and steel layers appear to have a relatively adhesive flow in zone between B and C. The Al layer experiences a reverse shear stress along the rolling direction, whereas the direction of the shear stress of the steel layer is the same as the rolling direction. The interfacial shear promotes the deformation of the steel layer while restrains the flow of the Al layer. Therefore, the thickness change is smaller for the Al layer than for the steel layer in zone between B and C. During the rolling process, the interfacial bonding strength is higher than the interfacial shear stress in zone between C and 0 and the Al and steel layers undergo a synchronous plastic deformation.

The minimum stable rolling reduction of 1060Al/AlSn20Cu/1060Al/steel LMC was explored by peeling a sample in the deformation zone and fracturing the Al layer with a higher rolling reduction. The fracture figures for the deformation zone are shown in Fig. 5. The thickness of the steel layer is 1.98 mm at the fracture position of the Al layer. The minimum stable rolling reduction is 40% (Fig. 4); therefore, the microstructure of the Al/steel clad sheets with single reductions of 35%, 46% and 57% is studied.

2.2 Interface microstructure of 1060Al/AlSn20Cu/1060Al/steel LMC

Fig.6 shows the BSE images and the element line scanning for the Al/AlSn20Cu and Al/steel bonding interfaces with different rolling reductions of 35%, 46% and 57%. No obvious defects or cracks are detected at the Al/AlSn20Cu and Al/steel interfaces, suggesting that the bonding interfaces are intact.

The EDS line scanning width is nearly unchanged, indicating that no obvious interfacial reaction layer is formed at the Al/steel interface. Wang et al[15], using high-resolution transmission electron microscopy (HRTEM), reported the

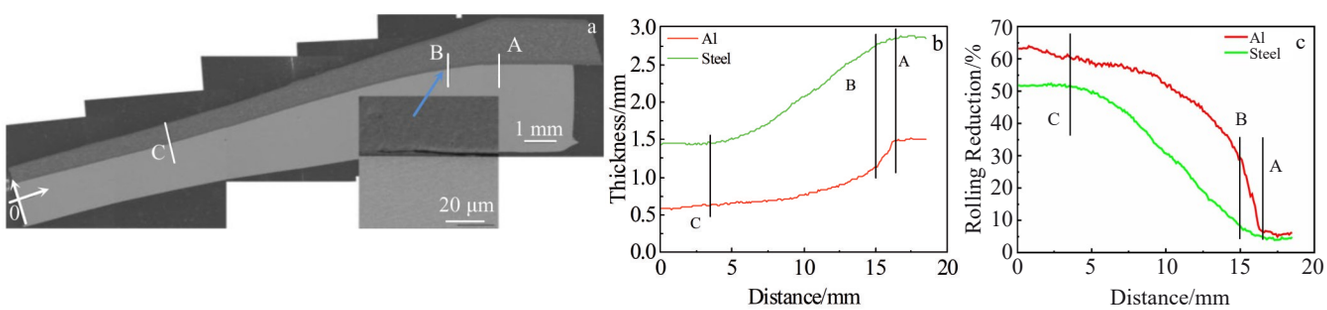

Fig.4 Interface morphology (a); thickness distribution (b) and rolling reduction (c) of deformation zones of 1060Al/AlSn20Cu/1060Al/steel LMC

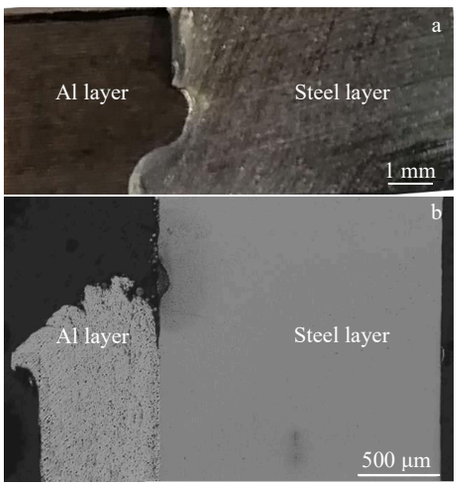

Fig.5 Fracture morphologies of deformation zone of 1060Al/AlSn20Cu/1060Al/steel LMC: (a) macro-fracture and (b) micro-fracture

formation of a diffusion layer of Al and Fe atoms with a dozen nanometres in thickness and amorphous layer with ~2 nm in thickness in the interface zone of sample with 50% rolling reduction. No visible diffusion layers are observed by SEM in the sample rolled with 57% rolling reduction (Fig. 6c). Increasing the rolling reduction decreases the thickness of the middle 1060Al layer.

Some small "sawtooth" gaps, similar to the Great Wall of China in shape, were observed at the Al/steel interfaces. The surfaces of the initial sheets are mechanically cleaned with a steel brush prior to rolling, and it is known that steel brushes not only clean surface impurities, but also generate hardening layers on the surfaces of matrix metals. During the rolling process, the surface hardening layers are cracked, fresh Al and steel are then squeezed into the cracks, where they are in contact and bonded during the rolling process. This phenomenon is reported in a previous study[16].

2.3 Microstructures of AlSn20Cu, 1060Al and steel layers

Fig. 7 shows the microstructure of the AlSn20Cu layer. It contains a Sn phase that is elongated along the rolling direction to form a white Sn ribbon with increasing rolling reduction. Compared to the Al alloy, the Sn metal has a smaller deformation resistance; consequently, it is elongated easily under the rolling pressure. When the samples are annealed at 300 – 400 °C, the Sn phase of the Al matrix is melted and becomes spheroidised[17].

The 1060Al layers show equiaxed grains (Fig. 8) with a grain size of 1–5 μm. The thicknesses of the 1060Al layer are 46, 62 and 80 μm. Compared to the 1060Al/AlSn20Cu clad sheet, the rolling reductions of the single 1060Al layer are 38.5%, 52.3% and 64.6%. The 1060Al undergoes drastic plastic deformation.

For the samples in this study, the contact surfaces between the Al and steel layers are brushed prior to roll bonding. Therefore, a considerable frictional shear force forms at the Al/steel interface during the rolling process. This interfacial shear force will produce an obvious strain and dynamic recrystallization in the 1060Al layer[18]. The interfacial fictional heat will also promote the formation and growth of fine equiaxed grains.

Fig. 9 shows the microstructure of the steel layers with different rolling reductions. Increased rolling reduction causes elongation of the grains along the rolling direction.

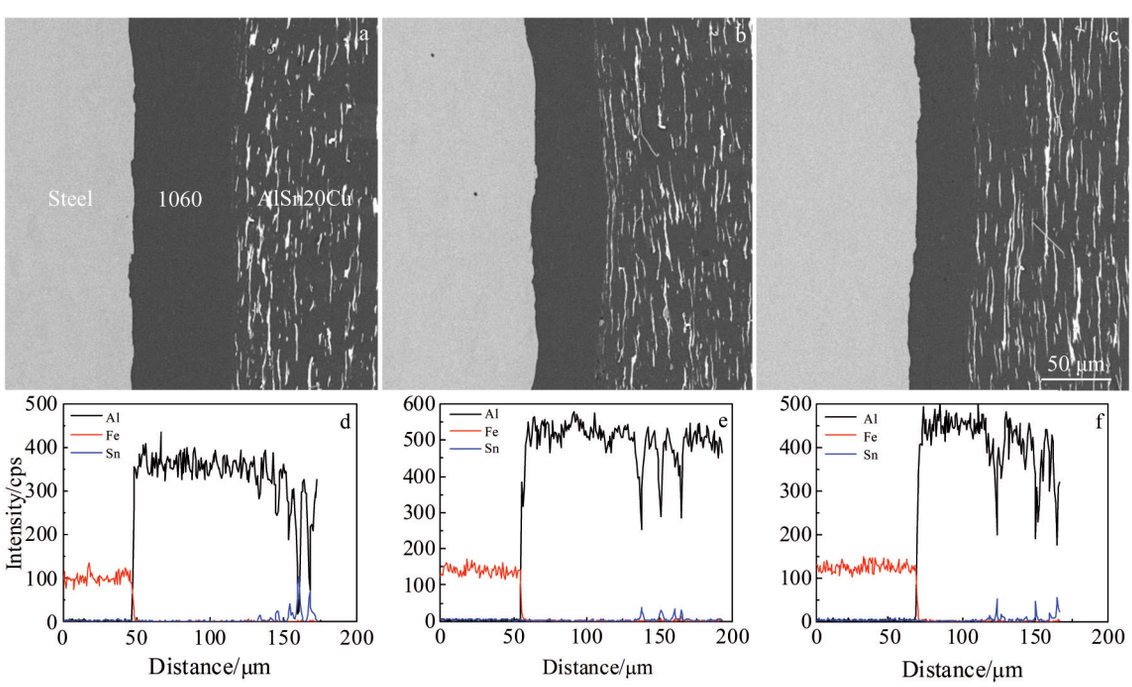

Fig.6 BSE images (a–c) and EDS line scanning results (d–f) of the interfaces of LMCs with different rolling reductions: (a, d) 35%, (b, e) 46% and (c, f) 57%

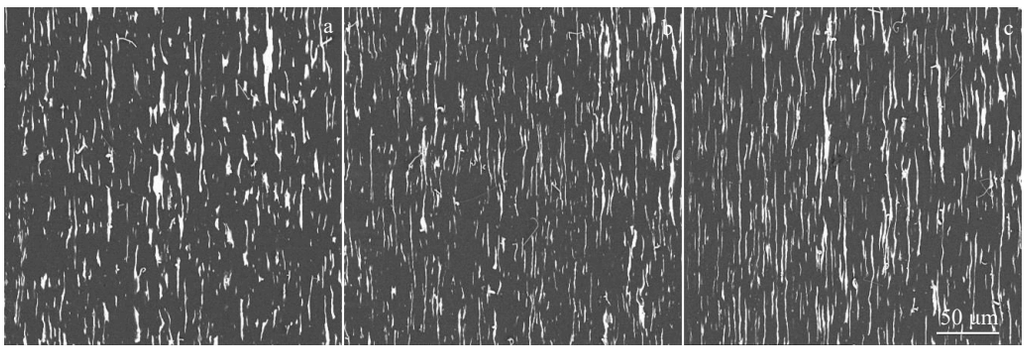

Fig.7 BSE images of AlSn20Cu layers for LMCs with different rolling reductions: (a) 35%, (b) 46% and (c) 57%

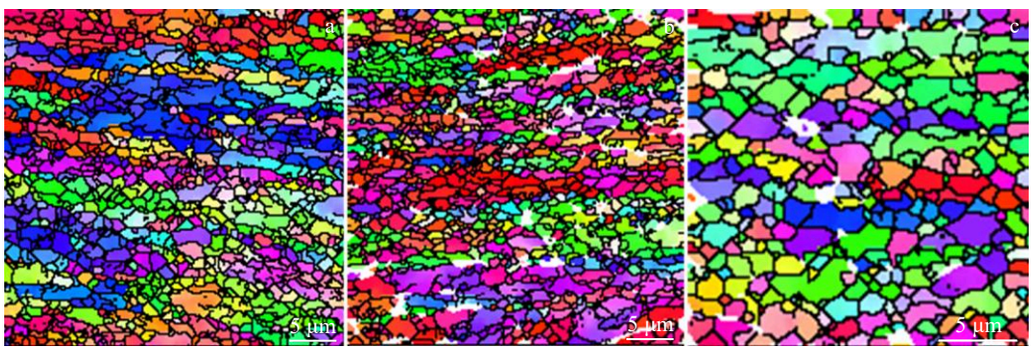

Fig.8 Microstructures of 1060Al layers with rolling reductions of 35% (a), 46% (b) and 57% (c)

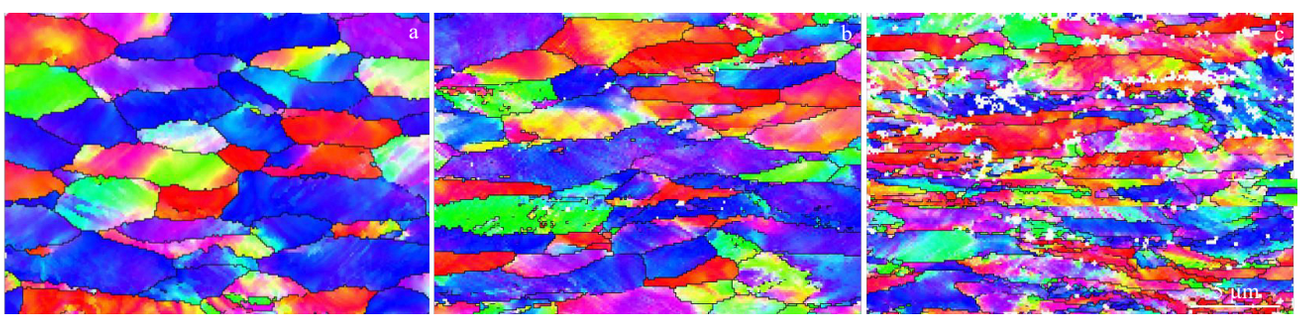

Fig.9 Microstructures of the steel layers with rolling reductions of 35% (a), 46% (b) and 57% (c)

During the rolling process, the steel layer experiences a large rolling pressure and the grains are deformed and elongated.

2.4 Mechanical properties of 1060Al/AlSn20Cu/1060Al/steel LMCs

Fig. 10 shows the mechanical properties of 1060Al/AlSn20Cu/1060Al/steel LMCs with different rolling reductions. The results of the tensile tests of the laminated sheets are listed in Table 3. The tensile strength increases, whereas the elongation decreases with increasing rolling reduction. This phenomenon is mainly related to the work hardening of the AlSn20Cu, 1060Al and steel layers. Notably, the stress-strain curve shows a stepwise drop (the black arrow in Fig.10) in the flow stress when the rolling reduction is 35%. Previous studies have attributed this sudden drop in stress to

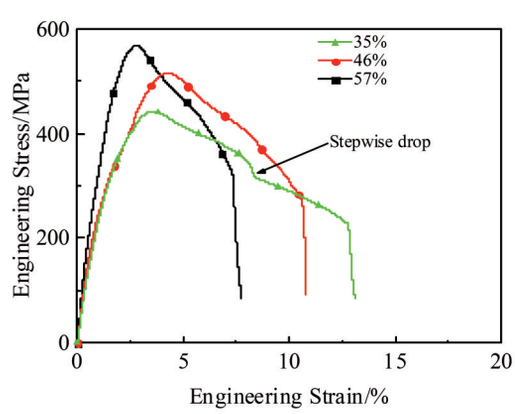

Fig.10 Engineering stress-strain curves of 1060Al/AlSn20Cu/1060Al/steel LMCs with different rolling reductions

the interfacial bonding strength[19–20].

Fig. 11 shows the tensile fracture morphologies of 1060Al/AlSn20Cu/1060Al/steel LMCs with different rolling reductions. The sample with 35% rolling reduction (Fig. 11a) shows independent delamination and deformation of the 1060Al/steel interface until fracture due to the weak interfacial bonding strength. Increasing the rolling reduction greatly minimizes the composite cracking until a final tensile fracture occurs.

The bonding strength of the Al/STS interface was studied by tensile shear tests (Table 3). The interfacial bonding strength increases with increasing rolling reduction. Fig. 12 shows the BSE images and EDS spectrum of the steel sides after the tensile shear tests with different rolling reductions. Two distinct contrast phases are evident in Fig. 12a and 12b. When the rolling reduction is 57%, a third contrast phase appears, as shown in Fig. 12c. The components of the three phases are analysed by EDS point analysis for the sample rolled with 57% reduction. The elements are Fe, Al and Sn. The area for Al increases with increasing rolling reduction. The Sn is observed in the Al layer with 57% reduction, indicating that the AlSn20Cu layer undergoes fracture during the tensile shear process.

The film theory holds that the contact of squeezed Al and steel contributes to the interface bonding of Al and steel layers[21–23]. The increasing rolling reduction will produce large roll pressure, thereby promoting the extrusion of base metals and expansion of the interfacial bonding area (Fig. 12). Therefore, the bonding strength of the Al/steel interface is improved with increasing rolling reduction. Due to its weak interfacial bonding strength, the sample with 35% rolling reduction shows a large crack between the 1060Al and steel layers (Fig. 11a). This difference in the cracking between the

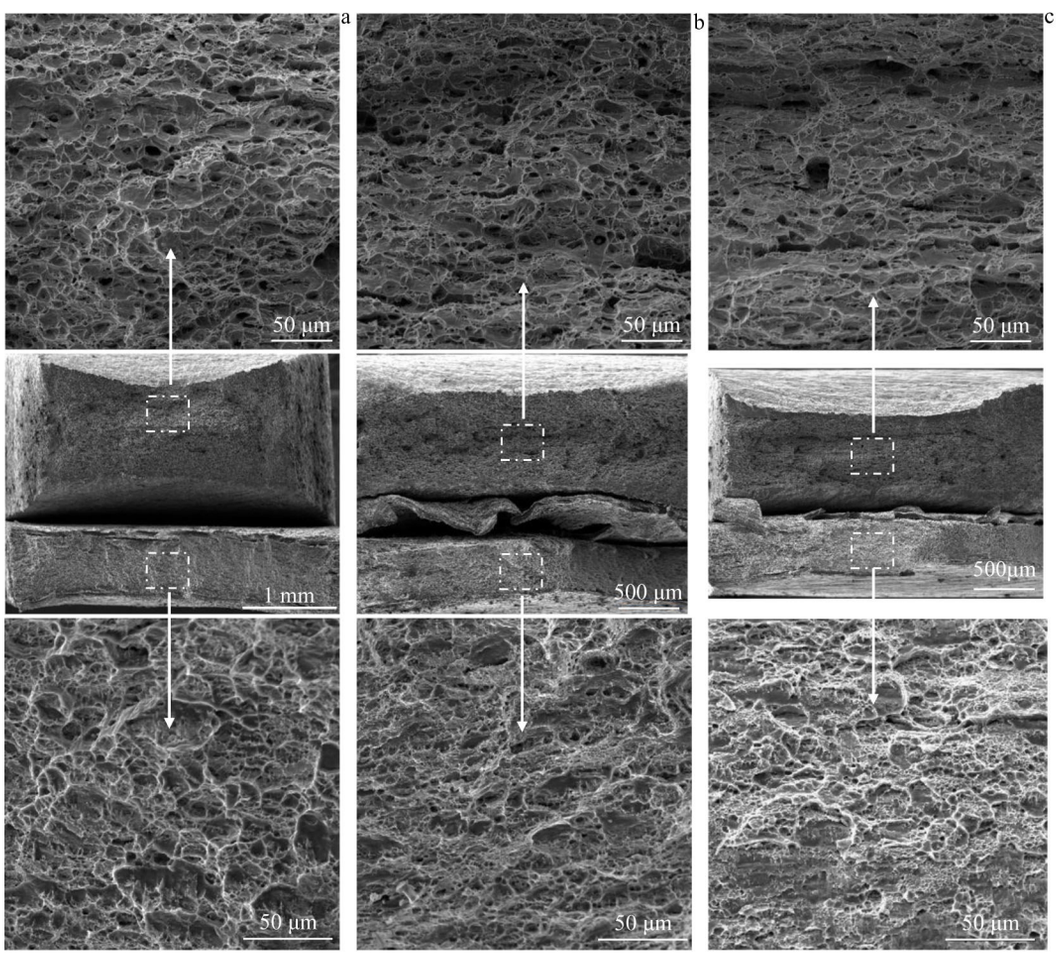

Fig.11 Fracture images after tensile tests of 1060Al/AlSn20Cu/1060Al/steel LMCs with different rolling reductions of 35% (a), 46% (b) and 57% (c)

Table 3 Mechanical properties of 1060Al/AlSn20Cu/1060Al/steel LMCs with different rolling reductions

Rolling reduction/%	Tensile strength/MPa	Yield strength/MPa	Elongation/%	Bonding strength/MPa
35	441	350	12.7	30
46	515	436	10.6	55
57	569	486	7.3	67

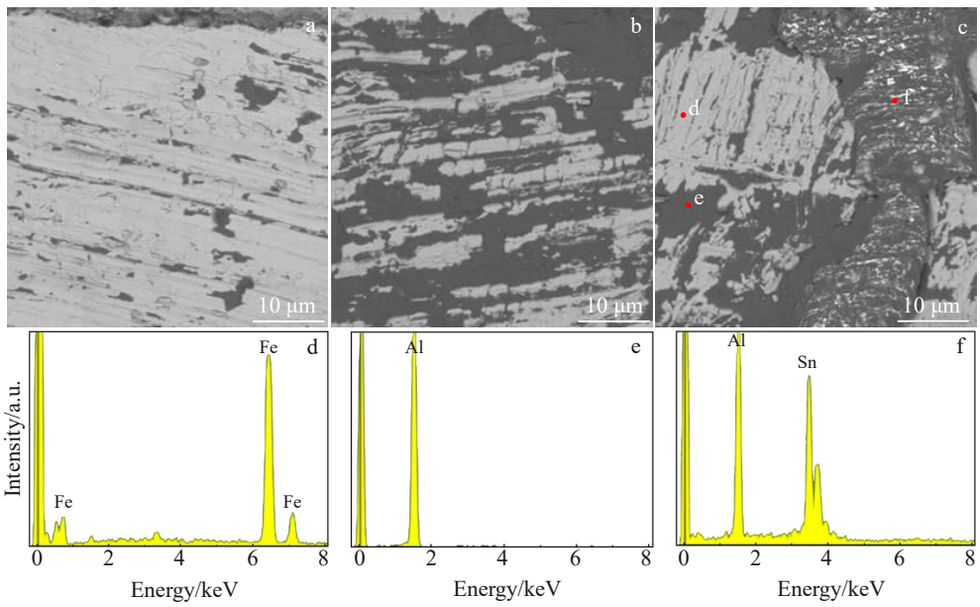

Fig.12 BSE images (a–c) and EDS spectra (d–f) of steel sides after tensile shear tests with different rolling reductions: (a, d) 35%, (b, e) 46% and (c, f) 57%

1060Al and steel interfaces can be explained by the sudden drop in stress observed in the stress-strain curve in Fig.10 for the 35% rolling reduction.

A number of dimples are evident in the magnified fracture figures of the AlSn20Cu and steel layers shown in Fig. 11. This indicates that the AlSn20Cu and steel layers undergo ductile fracture. Increase in rolling reduction decreases the size of the dimples and results in some cleavage steps. The smaller dimple size indicates that the samples absorb less energy in the serious plastic deformation. The cleavage steps indicate brittle fracture. Therefore, compared to other samples, the sample with 57% rolling reduction has the worst elongation.

We also explored the fracture mechanism of the AlSn20Cu layer with different rolling reductions by examining the local area from different imaging modes (Fig. 13). Some small pieces are observed on the walls and bottoms of the dimples (Fig. 13a, 13c, and 13e). Compared to the SEM images, the BSE images show different contrast (Fig.13b, 13d and 13f), as the small pieces are lighter in colour. The results shown in

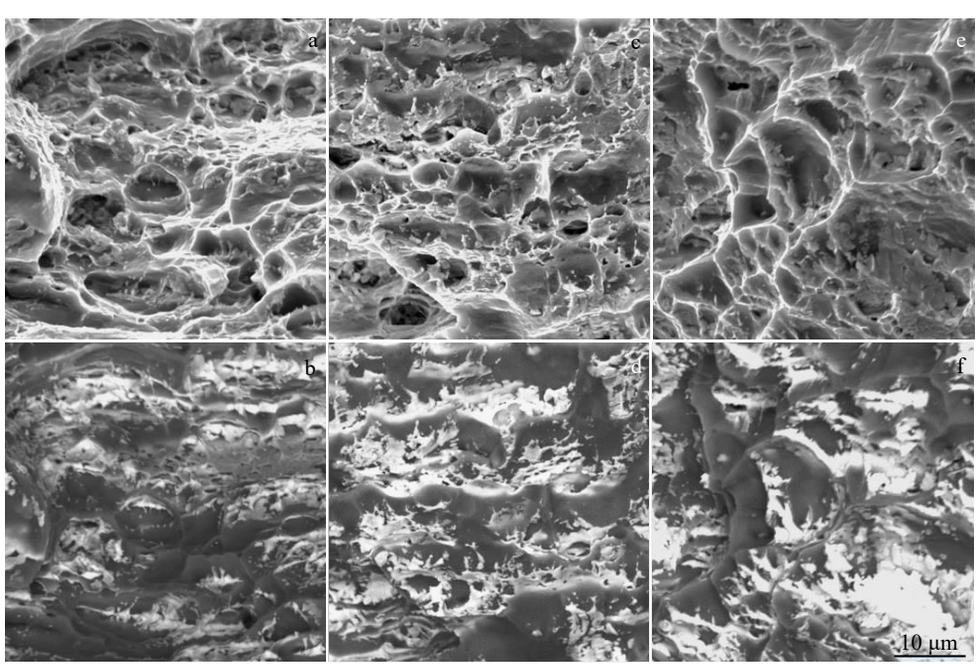

Fig.13 SEM images (a, c, e) and BSE images (b, d, f) of fracture morphologies of the same area in the AlSn20Cu layer with different rolling reductions: (a, b) 35%, (c, d) 46%, and (e, f) 57%

Fig.12 indicate that this lighter coloured phase is Sn metal.

During the plastic deformation of base metal, a concentrated stress forms between the base metal and heterogeneous particles[24–25] which causes the formation of micropores in the metal. The formation and linkage of the micropores then contribute to the ductile fracture. For the AlSn20Cu alloy, the Sn phase consists of heterogeneous particles. Therefore, the fracture of the AlSn20Cu layer is related to the Sn phase.

3 Conclusions

1) Laminated metal composites (LMCs) of 1060Al/AlSn20Cu/1060Al/steel are fabricated by cold roll bonding. According to observations of the deformation zone, the thickness variations of the Al and steel layers occur in three separate parts, and initial rolling reduction is 17%. After the peeling test, a minimum stable rolling reduction of 40% is obtained.

2) Due to the large rolling pressure, the Sn phases of the AlSn20Cu layer and the grains of the steel layers are elongated along the rolling direction with increasing rolling reduction. The frictional shear force of Al/steel interface is contributed to the equiaxed grains of 1060Al layer.

3) The tensile strength and interfacial bonding strength of the composite sheets increase, while the elongation decreases with increasing rolling reduction. This phenomenon is mainly related to the work hardening of AlSn20Cu and steel layers.

4) According to the fracture morphologies, the AlSn20Cu and steel layers show ductile fracture, and the fracture of the AlSn20Cu layer is related to the Sn phase.

References

1 Wang Z M, Yang Q, Sun Z P *et al*. *Materials Characterization*[J], 2020, 170: 110 684
2 Lu Z C, Gao Y, Zeng M Q *et al*. *Wear*[J], 2014, 309(1–2): 216
3 Lucchetta M C, Saporiti F, Audebert F. *Journal of Alloys and Compounds*[J], 2019, 805: 709
4 Wang G, Luo Z, Xie G *et al*. *Rare Metal Materials & Engineering*[J], 2013, 42(2): 387
5 Jamaati R, Toroghinejad M R. *Materials Science and Technology*[J], 2011, 27(7): 1101
6 Pohl P M, Kümmel F, Schunk C *et al*. *Materials*[J], 2021, 14(10): 2564
7 Manesh H D, Shahabi H S. *Journal of Alloys and Compounds*[J], 2009, 476: 292
8 Gao C, Li L, Chen X. *Materials and Design*[J], 2016, 107: 205
9 Filho A A M, Timokhina I, Molotnikov A *et al*. *Materials Science & Engineering A*[J], 2017, 705: 142
10 Kim Y K, Hong S I. *Materials Science & Engineering A*[J], 2019, 749: 35
11 Cui G M, Li X X, Zeng J M. *Advanced Materials and Processes Technology*[J], 2012, 217–219: 395
12 Li L, Gao C, Chen M Y *et al*. *Materials Research Innovations*[J], 2015, 19: 50
13 Wang C Y, Jiang Y B, Xie J X *et al*. *The Chinese Journal of Nonferrous Metals*[J], 2017, 27(4): 766 (in Chinese)
14 Manesh H D, Taheri A K. *Materials Science and Technology*[J], 2004, 20: 1064
15 Wang C, Jiang Y, Xie J *et al*. *Materials Science & Engineering A*[J], 2017, 708: 50
16 Wang P, Chen Z, Hu C *et al*. *Journal Materials Research and Technology*[J], 2020, 9(5): 11 813
17 Schouwenaars R, Torres J A, Jacobo V H *et al*. *Materials Science Forum*[J], 2007, 539–543: 317
18 Ma Y, Chi C. *Rare Metal Materials and Engineering*[J], 2016, 45(8): 2086
19 Wang P, Chen Z, Hu C *et al*. *Materials Science & Engineering A*[J], 2020, 792: 139 673
20 Hao X, Lu H, Nie H *et al*. *Journal of Alloys and Compounds*[J], 2020, 822: 153 608
21 Li L, Nagai K, Yin F. *Science and Technology of Advanced Materials*[J], 2008, 9(2): 23 001
22 Wu B, Li L, Xia C D *et al*. *Materials Science & Engineering A*[J], 2017, 682: 270
23 Lee K S, Bae S J, Lee H W *et al*. *Materials Characterization*[J], 2017, 134: 163
24 Chawla N, Chawla K K. *Metal Matrix Composites*[M]. New York: Springer, 2013: 370
25 Williams J J, Flom Z, Amell A A *et al*. *Acta Materials*[J], 2010, 58, 18: 6194

冷轧制备AlSn20Cu/钢多层板的微观组织和力学性能

王鹏举[1,2]，赵淑杰[2]，钟　宁[2,3]，杨　倩[2]，吴　波[2,3]，张　鹏[2]，杜　兵[2]，唐　倩[1]

(1. 重庆大学 机械与运载工程学院，重庆 400030)

(2. 重庆红江机械有限责任公司，重庆 402160)

(3. 重庆跃进厂有限公司，重庆 402160)

摘　要：通过室温冷轧制备出了1060Al/AlSn20Cu/1060Al/钢多层复合板材，并探索了轧制压下量对复合板微观组织和力学性能的影响。利用扫描电子显微镜和电子背散射衍射（EBSD）对复合板微观组织进行表征，通过拉伸试验测量了复合板力学性能。复合板的初始轧制压下量为17%，最小稳定压下量为40%。结果表明，随着轧制压下量的增加，铝合金层中锡相和钢中组织沿轧制方向被拉长，但是纯铝层呈现出等轴晶。随着轧制压下量的增大，复合板抗拉伸强度和界面结合强度增加，而延伸率下降。AlSn20Cu合金层的断裂主要跟其中的锡相有关。

关键词：轧制复合；AlSn20Cu/钢多层板；微观组织；力学性能

作者简介：王鹏举，男，1992年生，博士，重庆大学机械与运载工程学院，重庆 400030，E-mail：pjwang1992@126.com